Proliferation and differentiation of ductular progenitor cells and littoral cells during the regeneration of the rat liver to CCl$_4$/2-AAF injury

L. Yin, D. Lynch, Z. Ilic and S. Sell

Division of Experimental Pathology, Department of Pathology and Laboratory Medicine, Albany Medical College, Albany, NY, USA

Summary. Restoration of centrolobular injury induced by carbon tetrachloride (CCl$_4$), when hepatocyte proliferation is inhibited by treatment with N-2-acetylaminofluorene (AAF), is accomplished by proliferation of ductular progenitor cells, that arise intraportally and extend into the liver lobule. This pattern contrasts to the restitutive proliferation of hepatocytes when AAF is not administered, and the proliferation of non-ductular periportal oval cells follows periportal necrosis induced by allyl alcohol. The expanding ducts stain for alphafetoprotein (AFP), OV-6, pan-cytokeratin (CKPan), and laminin. The neoductular proliferation is accompanied by fibronectin-positive Kupffer cells and desmin-positive stellate (Ito) cells, which may play critical roles not only in controlling proliferation and differentiation of ductular progenitor cells, but also in reestablishing hepatic cord structure. When AAF is discontinued 7 days after injury, clusters of small hepatocytes appear next to the neoductules. Some of these small hepatocytes, as well as some larger hepatocytes adjacent to the ducts, stain for AFP and for carbamoylphosphate synthetase I (CPS-I), suggesting that the ductular progenitor cells may differentiate into hepatocytes when AAF is withdrawn. The restitutive process is facilitated by clearing of the central necrotic zone by infiltrating macrophages and co-migration of mature hepatocytes, with Kupffer cells and stellate cells, into the necrotic zone.

Key words: Liver stem cells, Oval cells, Ductular proliferation, Liver injury

Introduction

When proliferation of hepatocytes is inhibited, the loss of the remarkable ability of "mature" hepatocytes to proliferate and restore the liver mass after injury or partial removal (Grisham, 1962; Bucher, 1963; Bucher and Malt, 1971; Rabes et al., 1976; Engelhardt et al., 1984; Alison, 1986; Tournier et al., 1988; Lemire et al., 1991; Dabeva and Shafritz, 1993; Koch and Leffert, 1994), appears to be compensated for by involvement of liver precursor or stem cells (Sell et al., 1980; Sell and Leffert, 1982; Lombardi, 1982; Sell, 1990, 1994, 2001; Aterman, 1990; Alison et al., 1996, Sell and Ilic, 1997; Grisham and Thorgeirsson, 1997), that proliferate and differentiate into ductular cells or hepatocytes. Because the liver is normally able to reconstitute itself through proliferation of "mature" hepatocytes following 2/3rds partial hepatectomy of rats, or after injury with centro-lobular toxins (such as carbon tetrachloride (CCl$_4$)) and pan-lobular toxins (such as galactosamine), the presence of a more primitive regenerative cell in the liver was once considered unlikely (Grisham, 1962; Bucher and Malt, 1971; Rabes et al., 1976). However, more recent studies have identified a limited involvement of portal "stem cells" after centrolobular injury (Tournier et al., 1988; Lemire et al., 1991; Dabeva and Shafritz, 1993), and a more substantial involvement when hepatocyte proliferation is inhibited (Solt et al., 1977; Ghoshal et al., 1983; Ohlson et al., 1998; Petersen et al., 1998; Lindeman et al., 1999; Trautwein et al., 1999; Gijssel et al., 2000; Lindeman et al., 2000) or after severe liver injury induced by chemicals (Tournier et al., 1988; Lemire et al., 1991; Dabeva and Shafritz, 1993). In addition, reserve liver stem cells appear to be stimulated when liver injury is located periportally, such as after administration of allyl alcohol (AA) (Piazza, 1917; Thorgeirsson et al., 1976; Nostrant et al., 1978; Yavorkovsky et al., 1995). The zone of periportal

necrosis is restored by proliferation of small "null" periportal cells that sequentially acquire markers of differentiation of hepatocytes as the cells move from the intraportal space toward the undamaged mid- and central zones (Yavorkovsky et al., 1995). During this process, ultrastructural intermediates between non-descript cells, oval cells, transitional hepatocytes and hepatocytes are seen, with little or no ductal formation (Sell, 1997).

Active proliferation of small "oval cells" forming ductular structures after PH or chemical injury is markedly enhanced when proliferation of mature hepatocytes is inhibited, such as by feeding a choline deficient diet (Wilson and Leduc, 1958; Shinozuka et al., 1978; Sell et al., 1981) or administration of N-2-acetylaminofluorene (AAF) (Solt et al., 1977; Ghoshal et al., 1983; Petersen et al., 1998). Ghoshal et al. (1983) reported massive proliferation of oval cells after CCl_4 induced injury to the livers of rats pretreated with AAF. Hepatocyte proliferation began when AAF was removed from the diet and the liver returned to normal appearance within 14 days. Petersen et al. (1998) used inhibition by AAF to enhance oval cell proliferation after CCl_4 or AA injury, or partial hepatectomy. They concluded that, to see a true oval cell response, proliferation of hepatocytes must be inhibited. AAF inhibits proliferation of hepatocytes in mid-G1 (Ohlson et al., 1998; Lindeman et al., 1999; Trautwein et al., 1999; Gijssel et al., 2000; Lindeman et al., 2000). This block is associated with failure of elevation of cellular cdk2 and cyclin E levels after stimulation in comparison to control cells (Ohlson et al., 1998; Trautwein et al., 1999), reduced induction of cyclin D1-cdk4 complexes, and failure of the retinoblastoma protein to become hyperphosphorylated (Lindeman et al., 1999). Although there is an elevation of p21 (Trautwein et al., 1999) and reduced assembly of cyclin E-cdk2 complexes, the block is not related to binding by p21 (Lindeman et al., 2000). AAF does not affect these functions in oval cells (Trautwein et al., 1999). In contrast to inhibition of hepatocytes, proliferation continues in oval cells, as well as in preneoplastic nodules, which have low levels of p21 compared to surrounding hepatocytes (Gijssel et al., 2000). Thus, the initiation-promotion (Solt-Farber) protocol produces p53 dependent inhibition of hepatocytes, whereas so-called oval cells and cells in neoplastic foci are able to escape this inhibition. The present paper presents a more detailed immunohistochemical analysis of the involvement of non-parenchymal cells and extracellular matrix (ECM) components and the interaction of these elements with proliferating ductular cells and hepatocytes in the restitution of centrolobular injury induced by CCl_4 after AAF treatment. Early after CCl_4 injury, there is extensive periportal arborization of ductules and proliferation of ductal progenitor cells. When AAF is discontinued there appears to be rapid differentiation of ductular cells into small hepatocytes, as well as restoration of hepatocyte proliferation, which restore the liver cell mass. The central necrotic zone is reconstituted by migration of surviving mid-zone hepatocytes, along with nonparenchymal cells, after clearance of necrotic tissue by macrophages. Residual periportal ductular structures remain for as long as 2 months after injury. By 14 months small "foci" appear, suggesting a long time period for these "premalignant" changes to become manifest in the absence of an initiating event. The predominance of "ductal" oval cells is in marked contrast to non-ductular periportal oval cell proliferation after AA injury and suggests that different liver progenitor cells may respond to different injuries (Sell, 2001).

Materials and methods

Treatment of animals

Ten- to 11-weeks-old female Fischer 344 rats (Harlan, Indianapolis, IN) weighing 156-165g were used. They were maintained in a temperature-controlled room with a 12-hour light/dark illumination cycle. Rats were fed standard pelleted chow and had access to water *ad libitum*. To inhibit the proliferation of mature hepatocytes all rats received daily oral gavage of AAF (Sigma Chemical Co., St. Louis, MO) at a dosage of 10 mg/kg body weight for a period of up to 12 days. AAF was solubilized in a small volume of dimethyl sulfoxide (DMSO; Sigma Chemical Co.) and suspended in corn oil to a final concentration of 2 mg/ml. On day 5 of this regime, all rats were treated with CCl_4 (Aldrich Chemical Company, Inc., Milwaukee, WI) diluted in mineral oil at a dosage of 0.06 ml/100 g by oral gavage. These rats were killed under metofane (Mallinckrodt Veterinary, Inc., Mundelein, IL) anesthesia by exsanguination in groups of three at daily intervals up to 8 days after CCl_4 administration, and then at selected times up to 14 months after CCl_4 administration. All rats received a triple i.p. injection of [methyl-^{3}H]thymidine (70-86 Ci/mmol, Amersham Life Science Inc., Arlington Heights, IL) at 2 hours intervals at a dose of 3x1 mCi/kg body weight before sacrifice and cells synthesizing DNA were determined by autoradiography. Formalin-fixed and paraffin-embedded serial liver tissue sections (4 μm) were used for routine light microscopy (H&E staining), immunohistochemistry and autoradiography. All animal procedures were approved by the Albany Medical College Institutional Animal Care and Use Committee.

Primary antibodies

AFP, OV-6, CKPan, CPS-I, desmin, ED1, ED2, laminin and fibronectin antibodies were used in this study (Table 1). Polyclonal goat anti-rat AFP [goat # 89] was created and tested previously in our laboratory (Sell, 1973, 1978, 1983). AFP is the marker of fetal hepatocytes, beginning on embryonic days E10 and E11 in the rat (Sala-Trepat et al., 1979; Shiojiri et al., 1991) and ends at about 2 weeks after birth (Sell et al., 1976; Germain et al., 1988). AFP appears to be one of the

earliest markers of endodermal commitment toward liver cells (Sell et al., 1976; Sala-Trepat et al., 1979; Germain et al., 1988; Shiojiri et al., 1991). Monoclonal mouse anti-rat OV-6 antibody was produced against immunization with cells isolated from liver nodules induced by cyclic feeding of rats with AAF (Dunsford and Sell, 1989). OV-6 recognizes an epitope common to CK14 and CK19 (Bisgaard et al., 1993). CK14 is a marker of fetal hepatoblasts. Its expression begins at E12 and ends by E18 (Germain et al., 1988; Marceau, 1990, 1994; Marceau et al., 1992). CK14 stains oval cells (Bisgaard and Thorgeirsson, 1991; Bisgaard et al., 1993, 1994), and CK19 is expressed in both oval cells and biliary epithelium (Bisgaard et al., 1993). OV-6 stains both oval cells and bile duct cells (Dunsford and Sell, 1989; Dunsford et al., 1989), and is a good marker for early oval cell proliferation during chemical hepatocarcinogenesis (Dunsford et al., 1989), as well as for oval-like cells in human lesions (Crosby et al., 1998). Polyclonal rabbit anti-bovine CKPan was obtained from Zymed Laboratories Inc. (San Francisco, CA). This antibody reacts with bile duct epithelial cells in the rat liver. Polyclonal rabbit anti-rat CPS-I was a generous gift from Dr. W. H. Lamers, University of Amsterdam, The Netherlands (Lamers et al., 1984). CPS-I is the first enzyme of the urea cycle. The capacity of hepatocytes to synthesize CPS-I is present as soon as the cells become recognizable as hepatocytes (Geerts et al., 1994). Monoclonal mouse anti-porcine desmin antibody, clone DE-R-11 was purchased from DAKO Corporation (Carpinteria, CA). Desmin labels stellate (Ito) cells, smooth muscle cells, periportal fibroblasts and "Second-Layer Cells" of terminal hepatic venules in the liver (Dijkstra et al., 1985). ED1 and ED2 were the kind gifts of Dr. C. D. Dijkstra (Free University, The Netherlands). Both of them are mouse anti-rat monoclonal antibodies. ED1 recognizes a cytoplasmic antigen in circulating monocytes and small Kupffer cells in the liver. ED2 recognizes membrane antigens of large Kupffer cells in the liver but not monocytes (Dijkstra et al., 1985; Armbrust and Ramadori, 1996). Polyclonal goat anti-rabbit fibronectin and laminin antibodies were made in our laboratory as previously reported (Sell and Ruoslahti, 1982). Fibronectin is one of the noncollagenous glycoproteins in the liver produced by hepatocytes (Geerts et al., 1994; Rojkind and Greenwel, 1994). Fibronectin is localized in the space of Disse and was found diffusely in normal liver along the full length of the sinusoids in direct contact with hepatocyte microvilli (Sell and Ruoslahti, 1982; Rojkind and Greenwel, 1994). Laminins represent a family of multifunctional proteins of large molecular weight that are the major glycoproteins of basement membrane (Beck et al., 1990; Engel, 1991; Paulsson, 1992), and are mainly produced by stellate cells (Geerts et al., 1994; Rojkind and Greenwel, 1994). Laminin is localized to the endothelial lining of hepatic arteries, portal vein, and lymphatic vessels (Rojkind and Greenwel, 1994), is present predominantly in the basement membranes of blood vessels and bile ducts, and is only inconsistently seen lining the sinusoids in the normal rat liver (Sell and Ruoslahti, 1982). Laminin is also found in stellate cells (Ballardini et al., 1994) and smooth muscle cells of vessel walls (Rojkind and Greenwel, 1994).

Immunohistochemistry

Immunolabeling was carried out using streptavidin-biotin technique. Formalin-fixed and paraffin-embedded tissue sections (4 μm) were incubated in an oven at 55 °C for 1 hour and then deparaffinized in 3 changes of xylene and hydrated through 100% and 95% ethanol. The endogenous peroxidase activity was quenched by treatment with 2% H_2O_2 in methanol for 15 minutes at RT for all antibody staining except for ED1 and ED2. For ED1 and ED2 antibody labeling the slides were

Table 1. Details of the immunolabeling procedures

ANTIBODY TYPE (dilution)	ANTIGEN RETRIEVAL	DETERGENT	BLOCKIN NORMAL SERUM	SECONDARY ANTIBODY	CELL IDENTIFIED
AFP (gp; 1:800	EDTA*	saponin#	mouse	Mouse multi link §	oval
OV-6 (mm; 1:80)	EDTA	saponin	swine	swine multi link §§	duct/oval
CKPan (rp; neat)	EDTA	saponin	swine	swine multi link	duct
CPS-I (rp; :2500)	EDTA	saponin	swine	swine multi link	hepatocyte
Desmin (mm; 1:50)	EDTA	none	swine	swine multi link	Stellate
ED1 (mm; 1:1000)	pepsin**	none	goat	goat anti-mouse§§§	macrophage
ED2 (mm; 1:1000)	protease***	none	goat	goat anti-mouse	Kupffer
Fibronectin (gp; 1:100)	protease	none	mouse	mouse multi link	ECM
Laminin (gp; 1:250)	pepsin	none	mouse	mouse multi link	ECM

gp: goat polyclonal; mm: mouse monoclonal; rp: rabbit polyclonal. *: slides were boiled in the boiling ethylenediaminetetraacetic acid (EDTA) buffer (0.37 g EDTA was dissolved in 1 liter deionized water and pH adjusted to 8.0) for 15 minutes, cooled down to room temperature (RT), and washed 3 times in TBS buffer. **: slides were incubated with 0.4% pepsin A (Sigma Chemical Co.) in 0.01M HCl for 25 minutes at 37 °C followed by 3 washes of ice cold TBS. ***: slides were incubated with 0.05% protease type XIV (Sigma Chemical Co.) in TBS for 25 minutes at 37 °C followed by 3 washes of ice cold TBS. #: slides incubated with 0.1% saponin in TBS for 30 minutes at RT followed by 3 washes of TBS. §: biotinylated mouse anti-goat, guinea pig, rabbit, and sheep immunoglobulin (Sigma). §§: biotinylated swine anti-goat, mouse, and rabbit immunoglobulin (DAKO Corporation). §§§: biotinylated goat anti-mouse immunoglobulin (Sigma). ECM: extracellular matrix.

incubated for 1 hour at 37 °C in prewarmed Tris buffered saline (TBS, pH 7.2) containing glucose (180 mg%), sodium azide (6 mg%), and glucose oxidase (16.5 mg%) before applying the secondary antibody. Antigen retrieval was necessary for all immunostaining. To achieve the best availability of epitopes to the applied antibodies, different retrieval ways were used to expose different antigens. After antigen retrieval, the sections were incubated with free avidin and biotin (BLOCKING KIT, Vector Laboratories, Inc., Burlingame, CA) for 15 minutes at RT to prevent nonspecific staining due to endogenous biotin. The tissue sections were then blocked with 1% normal serum from the donor species of the secondary antibodies for 15 minutes at RT, followed by an one hour incubation with primary antibodies at RT. This was followed by an one hour incubation of 1% biotinylated secondary antibodies and a thirty minutes incubation of 1% ExtrAvidin-peroxidase (Sigma Chemical Co.) at room temperature. The reaction was developed with a saturated diaminobenzidine (DAB, free base; Sigma Chemical Co.) solution in 0.05 M Tris buffer (pH 7.6) containing 0.03% (v/v) H_2O_2. After immuno-histochemical staining, the sections were counterstained with Harris Modified Hematoxylin with Acetic Acid (mercury-free, Fisher Scientific, Springfield, NJ), dehydrated in alcohol, cleared in xylene and mounted with permount (Fisher Scientific). The specificity of the antibody-antigen reactions was tested by replacing the primary antibodies with normal sera from the donor species of the first antibodies. All of the normal sera and primary and secondary antibodies were diluted in 1% bovine serum albumin (BSA, Fraction V; Sigma Chemical Co.) in TBS. Thorough washing with TBS was performed between each step. In certain antibody stainings saponin was used to permeabilize the cell membranes. Table 1 provides details about primary antibodies and corresponding antigen retrieval methods, detergent, blocking normal sera, and secondary antibodies.

Histochemistry

Labeling of -glutamyl transpeptidase (GGT) was done on frozen sections as described by Rutenberg et al. (1969).

Autoradiography

Autoradiographic studies on formalin-fixed paraffin-embedded tissue sections (4 µm) were carried out in a darkroom with Kodak (Rochester, NY) No. 2 safe light filter as previously described (Sell et al., 1981). Deparaffinized sections were coated with half-strength Kodak NTB2 autoradiography emulsion (Eastman Kodak Company, New Haven, CT). The emulsion was exposed for 14 days at 4 °C, developed with Kodak D-19 developer for 3 minutes, washed in deionized water for 1 minute, followed by Kodak fixer for 5 minutes. The slides were then washed in deionized water and counterstained with Harris hematoxylin with acetic acid for 1 minute, dehydrated in alcohol, cleared in xylene and covered with permount. Tissue samples of the small intestine from the same animal were included on the same slide as one of the liver sections as a positive labeling control.

Slide evaluation

All the slides were evaluated blindly by two independent investigators.

Results

Because of the striking change that occurs when AAF is discontinued on day 7, and the marked involvement of different cell types during the early response, the results from days 1 to 7 after CCl_4 injury are presented first, followed by changes after day 7.

Hematoxylin and eosin and autoradiography

As shown in Figure 1A, on day 1 after injury, there are apoptosis, early necrosis and vacuolization of hepatocytes in the central zone (zone III) of the liver lobule. A few radiolabeled small mononuclear cells are present, mostly near the central vein (arrows in Fig. 1A). In the midzone (zone II) there is less than one radiolabeled hepatocyte or sinusoidal cell per 20x microscopic field, and essentially no detectable microscopic changes. No abnormalities are seen in zone I, but a few small radiolabeled intraportal "oval" cells in

Fig. 1. Autoradiography **(A-D)** and immunolabeling for OV6 **(E-H)**. **A.** Day 1. Early pericentral necrosis. Portal area is not injured. Arrows depict radiolabeled mononuclear cells close to the central vein (CV). Arrowheads indicate the intraportal proliferating cells. No radiolabeled midzone cells seen. x 20. **B.** Day 2. Increase in the number of radiolabeled mononuclear cells in the central area (arrows). Two radiolabeled hepatocytes (star) in the mid zone. x 20. Insert. Day 2. Marked increase in the number of intraportal proliferating cells. Much less number of cells in larger bile ducts (arrows) are labeled compared to the number of labeled cells in small ducts and in periductular cells (arrowheads). x 20. **C.** Day 3. Radiolabeled ductular cells move from intraportal to periportal zone (arrowheads) and midzone (arrows). Intraportal duct cells are no longer labeled. The labeled cells in the central area (CA) are in the macrophage lineage as shown by double labeling with ED1 and autoradiography (not shown). The hepatocytes lying between the ductules and the central area are not radiolabeled at this time. x 20. **D.** Day 7. There are essentially no labeled cells in the central area, which shows repair of injury. There is a shift of the radiolabeled ductular cells from the portal area to the ductules extending into the midzone (arrows). The cells in the intraportal ducts are not labeled. E-H, OV6. x 40. **E.** Day 1. Only bile duct cells are labeled (arrows). x 20. **F.** Day 4. New ducts (arrowheads) extending from portal area (PA) show much lighter labeling than preexisting bile duct cells (arrows). x 20. **G.** Day 4. OV6 positive cells approach central area (CA) forming either ductular structure or as individual cells connecting to the hepatic cords (arrows). x 40. **H.** Day 7. OV6 positive cells in neoductules extend from the portal area into the midzone (arrows). CV: central vein; PV: portal vein; CA: central area; PA: portal area. x 20
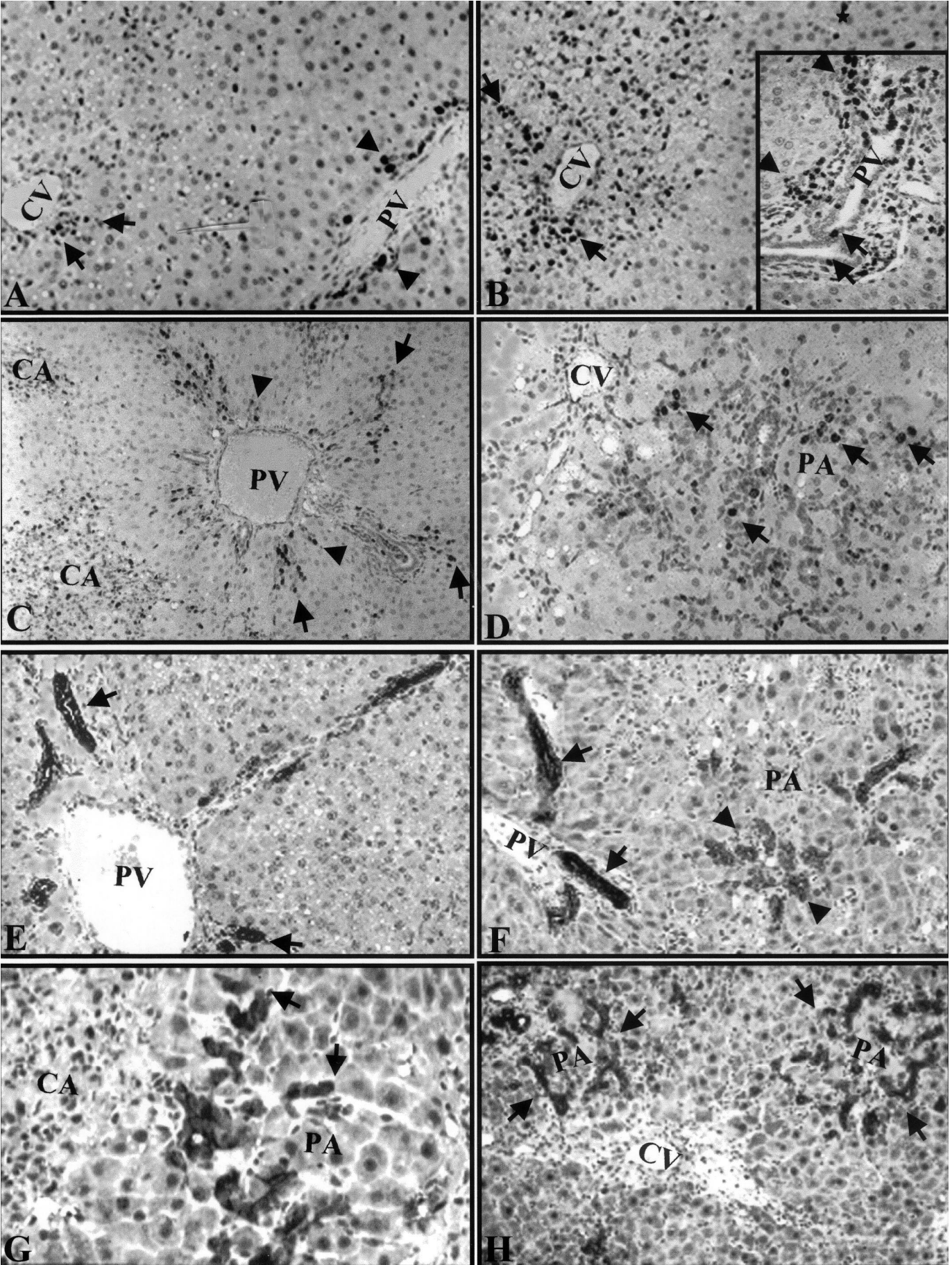
the ducts and next to the ducts are obvious (arrowheads in Fig. 1A). By day 2 (Fig. 1B), the cellular architecture of the hepatocytes in the zone 3 is lost and replaced by acellular spaces (fluid) mixed with mononuclear cells and some erythrocytes. The hepatocytes in zone 2 adjacent to the necrotic central zone are vacuolated. Many more small mononuclear cells are now labeled in zone III (about 50%, arrows), but very few hepatocytes (star) or sinusoidal cells are labeled in zone II. This is in marked contrast to rats treated with CCl_4 only, in which large numbers of radiolabeled hepatocytes are seen in the midzone by day 2 after injury (result not shown). There is a marked increase in labeled ductular and intraportal periductular cells (inset, Fig. 1B). Smaller ductules and terminal duct cells (TDC) (arrowheads) are more highly labeled than larger ducts (arrows). By day 3 after injury, proliferating ductular cells extend into the adjacent periportal zone (zone I) and the intraportal ducts contain very few labeled cells (Fig. 1C). The midzone contains a few labeled sinusoidal cells and hepatocytes, but these are relatively rare compared to other zones. The central necrotic zone is now more cellular, filled with small mononuclear cells, with about 30% of these radiolabeled. From days 4 to 7, there is a marked decrease of labeled cells in the necrotic central zone, which becomes much smaller. There is the appearance of compression of the radiolabeled mononuclear cells against the central vein so that by days 6 or 7 there are no labeled cells in zone III (Fig. 1D). The labeled ductular cells now extend further across the midzone to lie almost against the central vein in some fields or approaching the remainder of the cellular pericentral remnant of the necrotic zone (arrows in Fig. 1D). The ducts become branched and "arborized" as they move across the midzone, with clear radiolabeling of TDCs, whereas the number of labeled cells in the intraportal region actually decreases so that few are seen after day 6. On day 6 and 7 there are a few small hepatocytes next to the expanding ductules. From day 8, one day after AAF is discontinued, until day 10, there is a massive expansion of this population of small hepatocytes (see below).

Specific markers

The expression of specific markers will be described in the following order: 1) those seen in cells arising in the intraportal zone and extending into the portal zone;

2) those in cells in the central necrotic zone; 3) those in both the portal and central zones; 4) extracellular markers and 5) hepatocyte markers.

Cells arising intraportally

OV-6 and CKPan label preexisting bile ducts, ductules, terminal duct cells, and proliferating neoductules with essentially the same pattern. At days 1 and 2 there is staining of ducts only, including canals of Hering and terminal duct cells (Fig. 1E, arrows). There is no central or midzone staining. After day 3 small ducts extend from the intraportal zone into the periportal zone with increasing spreading and arborization (Fig. 1F, arrowheads). Preexisting ducts (arrows) stain more strongly than new ducts (arrows, Fig. 1F). At days 4 and 5 multiple small ducts extend into the midzone. Terminal duct cells are readily identifiable with positive TDC located next to negative hepatocytes (arrows in Fig. 1G). By days 6 and 7 there is further extension of ductular structures across the hepatic lobule and they surround the repairing central areas, in some instances within a few cell layers of the central vein (Fig. 1H). Both the intraportal ducts and expanding periportal ductules stain for OV-6 and CKPan, with the intraportal ducts consistently showing stronger staining..

AFP also stains arborizing ducts, but with a significantly different pattern than OV-6 and CKPan. There is little, if any, staining of larger preexisting intraportal ducts. However, some of the cells in the ductules extending out of the intraportal zone are positive. On day 1, occasional periductular small oval cells and small intraportal ductular cells in groups of 3 to 6 are positive (Fig. 2A). The positive cells are also seen after CCl_4 only treatment, but are less frequent, and may easily be distinguished from eosinophils, which are infrequently also seen in intraportal zones (result not shown). By day 2 many small TDCs and periductular oval cells are positive, as are occasional cells in larger ducts. The insert in Fig. 2A shows AFP+ mitotic cells. On days 3 to 7 the AFP positive oval cells increase in number and expand toward the injured central zone either as ductular structures (arrows, Fig. 2B) or as individual oval cells (arrowheads, inset of Fig. 2B). Rare hepatocytes are also faintly positive. As the small ducts expand into the lobule, fewer cells in the intraportal ducts are positive and the larger ducts with intestinal metaplasia show few labeled cells, but the expanding

Fig. 2. Immunolabeling for AFP **(A-D)** and ED1 **(E-H)**. **A.** Day 1. Very few intraportal AFP positive cells. Insert. Day 2, x 20. Mitotic AFP positive oval cells in portal region (arrowheads). x 20. **B.** Day 3. The number of AFP positive oval cells increase in the periportal area forming ductular structures (arrows) or as individual cells (insert, x 20, arrowheads). The pericentral zone shows necrosis. x 20. **C.** Day 7. AFP positive new ducts move from portal zone toward central zone (arrows). Intraportal bile ducts are negative for AFP. The arrowheads in the insert show AFP positive terminal duct cells adjacent to AFP negative small hepatocytes. x 20. **D.** Day 7. Two clusters of AFP Positive neoductules (arrows) surround the repairing central zone. x 20. **E.** Normal rat liver. Small round cells (macrophages) in the sinusoids are labeled (arrows). x 40. **F.** Day 1. Scattered ED1 positive cells in the necrotic zone adjacent to the central vein and at the edge of necrotic zone (arrows). A few ED1 positive cells are also seen in intraportal area. x 20. **G.** Day 4. The central necrotic zone is heavily infiltrated with ED1 positive cells (arrows). x 40. **H.** Day 6. ED1 positive macrophages in the shrinking central necrotic zone (arrows). A few ED1 positive cells admixed with many negative portal oval cells (arrowheads). x 20. CV: central vein; PV: portal vein; CA: central area; PA: portal area; Bd: bile duct.
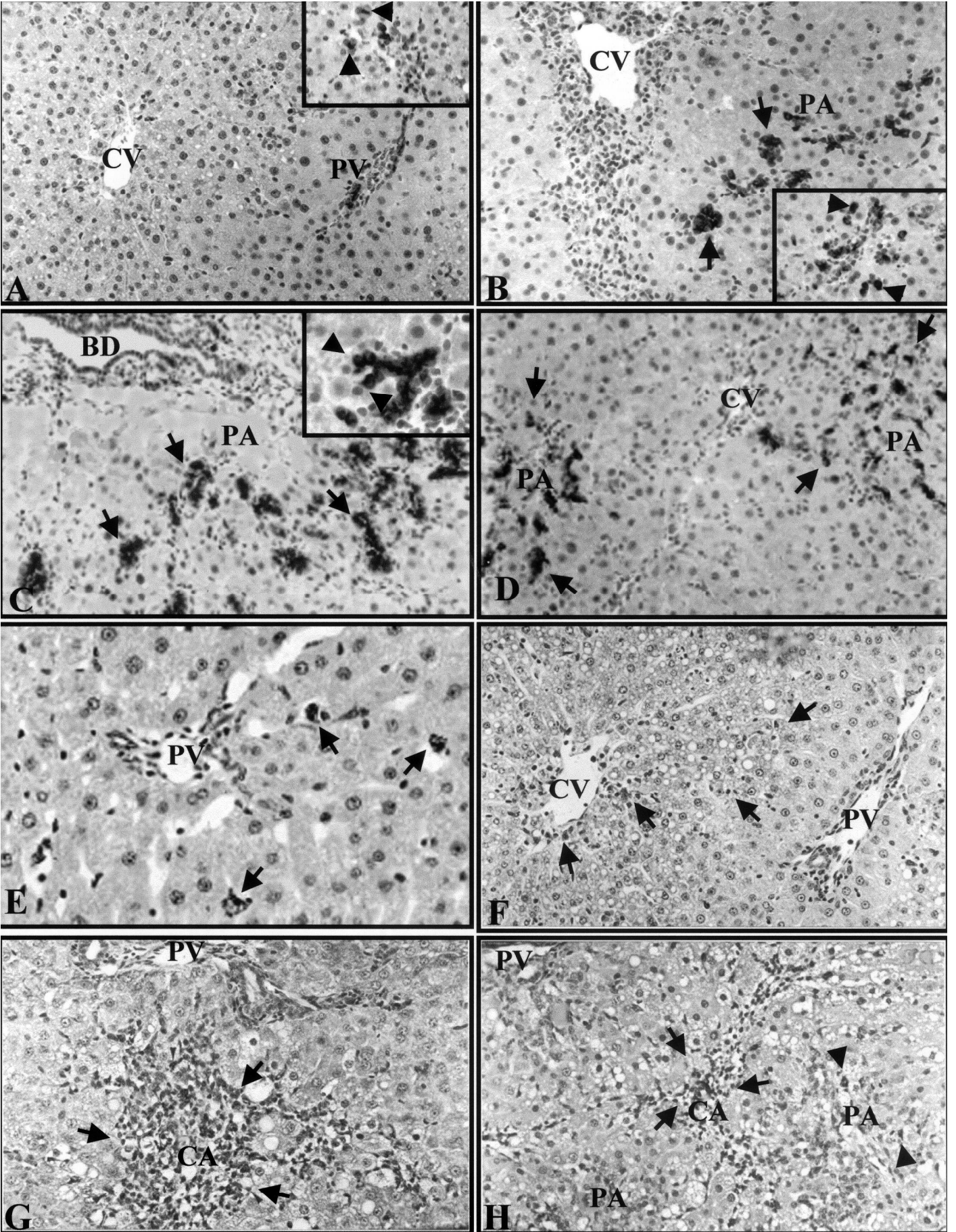
ductules in the midzone remain positive (Figure 2C). The insert in Fig. 2C shows AFP+ TDCs adjacent to AFP- small hepatocytes. By day 7 up to 2/3rds of the hepatic lobule is occupied by AFP+ ductules (arrows, Fig. 2D).

Cells in central zone (Zone III)

ED1 stains rare rounded cells in the sinusoids with a granular cytoplasmic staining pattern in normal liver (arrows, Fig. 2E). Infiltration of ED1 labeled macrophages into the central necrotic zone is first seen on day 1 after CCl_4 treatment (Fig. 2F, arrows), peaks on days 3 and 4 (Fig. 2G), and declines thereafter (Fig. 2H). On day 1, ED1+ cells are seen mainly adjacent to the central vein and at the margin of the central and midzone (Fig. 2F), delineated by vacuolated central hepatocytes (incipient necrotic cells). There are also a few scattered ED1+ cells in the paracentral area intermingled with vacuolated hepatocytes. By day 2 there are many more positive cells throughout the necrotic cells in the central zone. These cells are smaller than ED2+ cells (see below) and many have prominent vacuoles. Some mitotic cells in the central zone are ED1 positive and some mitotic figures are negative. On days 3 and 4 there are increasing numbers of ED1+ cells in the central zone, so that most of the pericentral cells are now ED1+ (arrows, Fig. 2G). However, very few portal cells are ED1+. On days 5-7 the number of ED1+ cells in the central necrotic zone decreases markedly as the necrotic zone diminishes. By day 7 most central zones have a thin layer of ED1+ mononuclear cells around the central vein (arrows, Fig. 2H). There are very few ED1+ cells around the expanding ducts (arrowheads, Fig. 2H). After day 10, ED1 staining is limited to a few intraportal, sinusoidal and pericentral mononuclear cells.

ED2 stains large spindle-like cells in the sinusoids (Kupffer cells) in the normal rat liver (Fig. 3A). ED1+ cells are smaller and have more prominent vacuoles than ED2+ cells. On days 1 to 2, ED2+ cells are markedly enlarged and concentrated at the margin of the necrotic central zone and the surviving hepatic lobule (arrows, Fig. 3B). Positive cells lying within the necrotic zone lose cellular definition and become smudged, suggesting dissolution of these cells in the central zone (arrowheads, Fig. 2B). On days 3-4, there is a marked increase of positive cells in the central zone, whereas there are very few positive cells in the portal zone (arrowheads, Fig. 3C). By day 6-7, the central necrotic zones have become almost completely repaired and there are only a few residual ED2+ cells (arrows, Fig. 3D) and a few ED1+ small round cells (Fig. 2H), which are most likely surviving macrophages. After day 7, ED2+ cells are typical spindle shaped sinusoidal cells and are occasionally also seen in clusters of small hepatocytes in a pattern similar to fibronectin labeling (see below).

Cells in both portal and central zones

Desmin stains smooth muscle cells of the blood vessels (arrow, Fig. 3G) and dendritic cells around the bile ducts and vessels (arrowheads, Fig. 3G), but not sinusoidal cells in normal rat liver. However, by 2 days after CCl_4-induced injury, desmin+ cells increase in number in both central (dashed arrow, Fig. 3F) and portal zones (short arrows, Fig. 3F). In addition, small sinusoidal cells (stellate cells) become positive for desmin (arrowheads, Fig. 3F). These cells are considered to be "activated". Desmin+ cells are dendritic (stellate) and very different in appearance form ED1 or ED2 positive cells. There appears to be different fates for central zone and portal zone stellate cells. The number of desmin+ central stellate cells peaks on days 3 and 4 after injury in the central zone (arrows, Fig. 3G) and then decreases. By day 7, desmin+ cells become far less prominent and limited to a few granular cells around the central vein (broken arrows, Fig. 3H). The fate of the central stellate cells is similar to that of the central ED1+ macrophages and ED2+ Kupffer cells. As the central stellate cell number decreases, there is an increase in portal stellate cells (arrows, Fig. 3H). On days 3-4, increasing numbers of desmin+ cells are seen in the portal zone (dashed arrows, Fig. 3G). By day 7, the number of desmin+ portal stellate cells is further increased (Fig. 3H). There is an organized meshwork arrangement of strongly desmin+ stellate cells associated with expanding ductular structures in the portal zone.

Extracellular matrix

Fibronectin is localized in the space of Disse in the normal liver and also in spindle shaped sinusoidal cells (Kupffer cells). In general, the cellular staining for fibronectin in the normal liver is very similar, if not

Fig. 3. Immunolabeling of ED2 **(A-D)** and Desmin **(E-H)**. **A.** Normal rat liver. ED2 positive spindle-like sinusoidal Kupffer cells (arrows). x40. **B.** Day 2. Enlarged ED2 positive cells at the edge of central necrotic zone (arrows) and fragmented ED2 positive cells within the necrotic area (arrowhead). x 20. **C.** Day 3. ED2 positive Kupffer cells increase in number and infiltrate into the necrotic central area (arrows). Very few ED2 positive cells seen in the portal area (arrowheads). x 20. **D.** Day 7. A thin layer of ED2 positive Kupffer cells in the repairing central zone (arrows). x 40. **E.** Normal rat liver. Smooth muscle cells of blood vessels (arrow), dendritic cells around the bile ducts and portal vein (arrowheads) are desmin positive. No desmin positive sinusoidal cells are seen. x 40. **F.** Day 2. Increase in number of desmin positive stellate (Ito) cells in necrotic zone (arrows) and uninjured portal area (broken arrow). Sinusoidal stellate cells now express desmin (arrowheads); "activated" stellate cells express desmin. x 20. **G.** Day 3. Further increase in number of stellate (Ito) cells in both the central necrotic zone (arrows) and uninjured portal area (broken arrows). A small number of sinusoidal cells in midzone (arrowheads). x 20. **H.** Day 7. Decrease in number of central stellate cells along with the central repair (broken arrows). Significant increase of stellate cells around the ductular portal oval cells (arrows). x 20. CV: central vein; PV: portal vein; CA: central area; PA: portal area; BD: bile duct; A: artery.
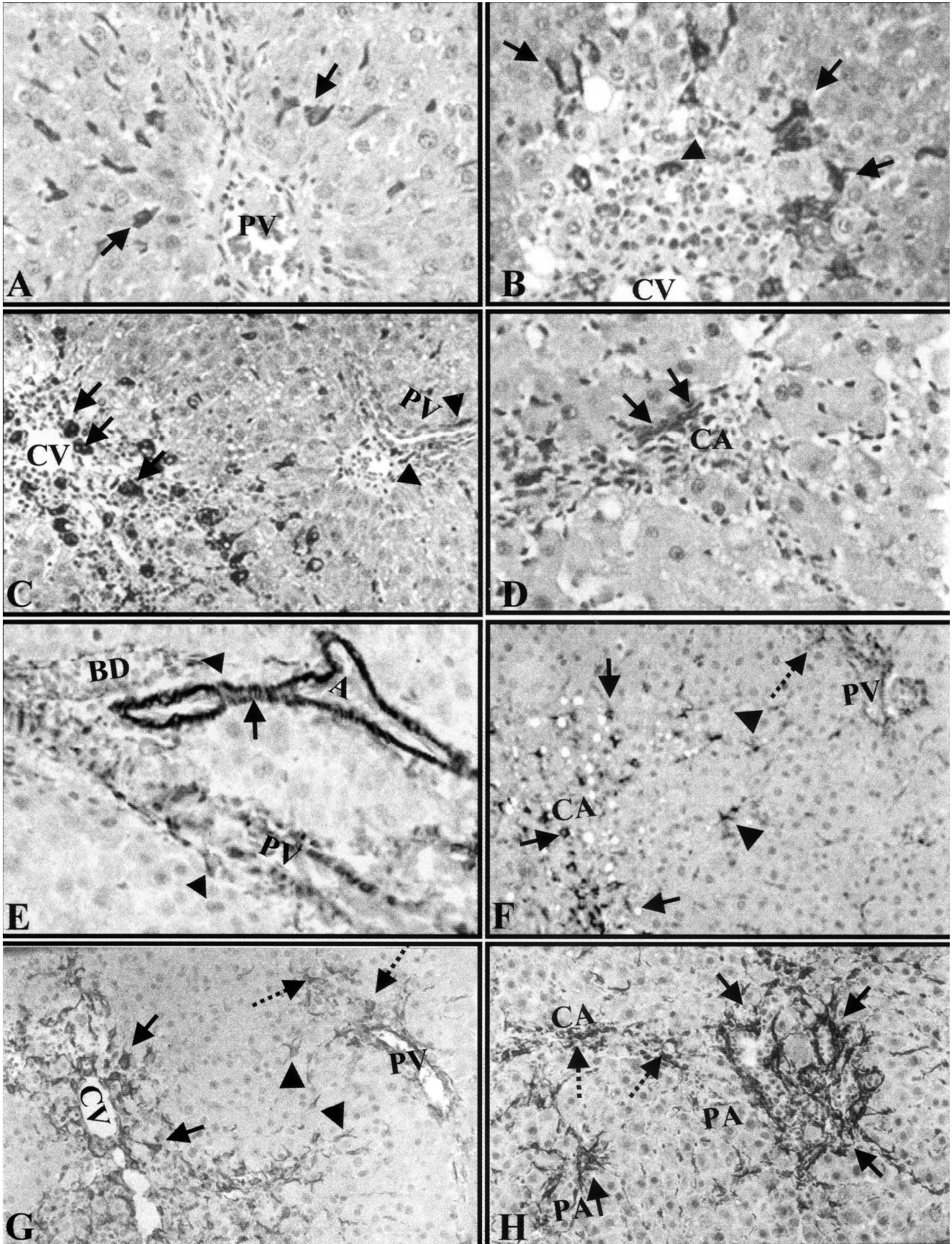
identical, to that of ED2. On day 1 after injury, fibronectin+ cells are enlarged and prominently located at the margins of the necrotic central zone (arrows, Fig. 4A). A few positive cells in the necrotic zone appear fragmented. By days 2 and 3, fibronectin+ cells increase further at the edge of the necrotic zone and there is a general decrease of fibronectin staining in the sinusoids of the midzone (Fig. 4B). Recovery of normal sinusoidal fibronectin expression occurs by day 4 (not shown). Fibronectin decreases as repair of the central zone progresses. By day 7, only a few fibronectin positive cells can be seen around the central vein (arrowheads, Fig. 4C). The number of fibronectin+ cells among the expanding portal ductules is much less than the number of stellate cells (arrows, Fig. 4C). After day 8 fibronectin positive cells are essentially limited to spindle cells in the sinusoids, although a few positive cells are seen in clusters of small hepatocyte (see below).

Laminin is normally located around bile ducts and blood vessels, as well as in the sinusoids (normal not shown). During the first day after injury there is dissolution and fragmentation of laminin around ducts and vessels in the intraportal zone (result not shown). On days 2 and 3, there is an increase of triangular laminin+ sinusoidal cells with a granular staining pattern in the central necrotic zone (arrows, Fig. 4D). These laminin+ cells decrease in number after day 3 and are rarely seen after day 5 (Fig. 4E). Meanwhile, there is an increasing number of laminin+ cells around the newly appearing portal ductules, so that by day 5 newly sprouting ducts as well as individual oval cells are laminin positive. The expanding ducts acquire a more organized structure with surrounding laminin (arrows, Fig. 4E), so that by days 6 and 7 the well-formed ducts in the hepatic lobules are delineated by a laminin layer. In general, the distribution of laminin+ cells is similar to that of desmin+ stellate cells.

Hepatocyte Marker

CPS-I positive hepatocytes are found scattered throughout the liver, but more frequently in a periportal location in the normal liver. On days 1 and 2, there are some CPS-I positive surviving hepatocytes in the necrotic central zones intermingled with CPS-I negative nonparenchymal cells (macrophages, Kupffer cells and stellate cells (arrows, Fig. 4F) and cellular debris (arrowheads, Fig. 4F). Most of the CPS-I+ cells are vacuolated, suggesting some injury. A few positive

hepatocytes remain in the portal zone, but they are fewer than in normal liver. On days 3 and 4, CPS-I+ hepatocytes are no longer seen in the central necrotic zone, but a layer of positive cells is prominent at the margin of the necrotic zone and the surviving midzone (arrows, Fig. 4G). There are more CPS-I+ cells at the edge of the portal zone (arrowheads, Fig. 4G). Portal zone hepatocytes are negative, except for some elongated cells next to proliferating ducts (arrows, Fig. 4G). This becomes more pronounced on days 5 and 6, when some portal cells next to newly forming ducts are positive. These are more rounded and appear to be small hepatocytes (transitional hepatocytes?) (arrows, Fig. 4H). Later, these cells increase in number and are prominent at the junction of the ductules and the margin of the remaining central hepatocytes (see below).

Changes after Day 7

After AAF is discontinued on day 7, many clusters of small basophilic hepatocytes (usually less that 25 cells per cluster) are seen, usually in the midzone between the midzonal ductules and the central hepatocytes (Fig. 5A,B). Mitotic figures are easily identified both in the small hepatocytes in the clusters and in the larger "mature" hepatocytes in the midzone. By day 14, the number of small hepatocytes decreases and there is an increase in intermediate sized hepatocytes in the midzone as the structure of the liver lobule is largely restored. After day 18, small hepatocytes are difficult to identify, and the number of ductular cells gradually decreases. Using OV-6 and CKPan, well formed ductules can be seen extending into the midzone, but not into the central zone on days 18-28. From day 7 to day 10, about 1 or 2 in 20 of the small hepatocytes in the clusters is radiolabeled in autoradiographs (Fig. 5C), and there are 4 to 10 labeled large hepatocytes per 20X field (Fig. 5D). After day 18, there are few if any labeled ductular or small hepatocytes, but the number of labeled mature hepatocytes remains at about 4 to 10 per 20x field. From days 9 to 28, there is a decrease in AFP staining of ductules, so that by day 28 only rare ductule cells are weakly positive. Some of the small hepatocytes stain for AFP (Fig. 5E) or OV-6 (Fig. 5F), and most are CPS-I positive (Fig. 5G). On days 10-18, there are occasional hepatocytes immediately adjacent to ductules in the periportal zone that are weakly positive for AFP.

At two months after injury there is residual extension of well formed ductules into immediate

Fig. 4. Immunohistochemistry for fibronectin **(A-C)**, laminin **(D, E)** and CPS-I **(F-H)**. **A.** Day 1. Fibronectin positive cells are enlarged and concentrated at the edge of necrotic area (arrows). The arrowheads point to fragments of stained cells in the necrotic zone. x 40. **B.** Day 2. Increase in number of fibronectin positive cells in central zone (arrows). x 40. **C.** Day 7. Fibronectin positive cells intermingle with portal oval cells (arrows). A thin layer of fibronectin positive cells at the edge of the repairing central zone (arrowheads). x 40. **D.** Day 2. Laminin positive triangular cells in the necrotic area (arrows). x 40. **E.** Day 5. Laminin surrounds expanding portal oval cells forming neoductules (arrows). x 40. **F.** Day 1. CPS-I positive hepatocytes in necrotic central zone including surviving (arrows) and fragmented (arrowheads) hepatocytes. x 20. **G.** Day 3. Decrease of central CPS-I positive cells. CPS-I positive cells concentrate at the edge of central necrotic zone (arrows) and the edge of portal proliferating cells (arrowheads). x 20. **H.** Day 6. Transitional CPS-I small hepatocytes among portal proliferating cells (arrows). x 20. CA: central area; CV: central vein; PV: portal vein; PA: portal area.
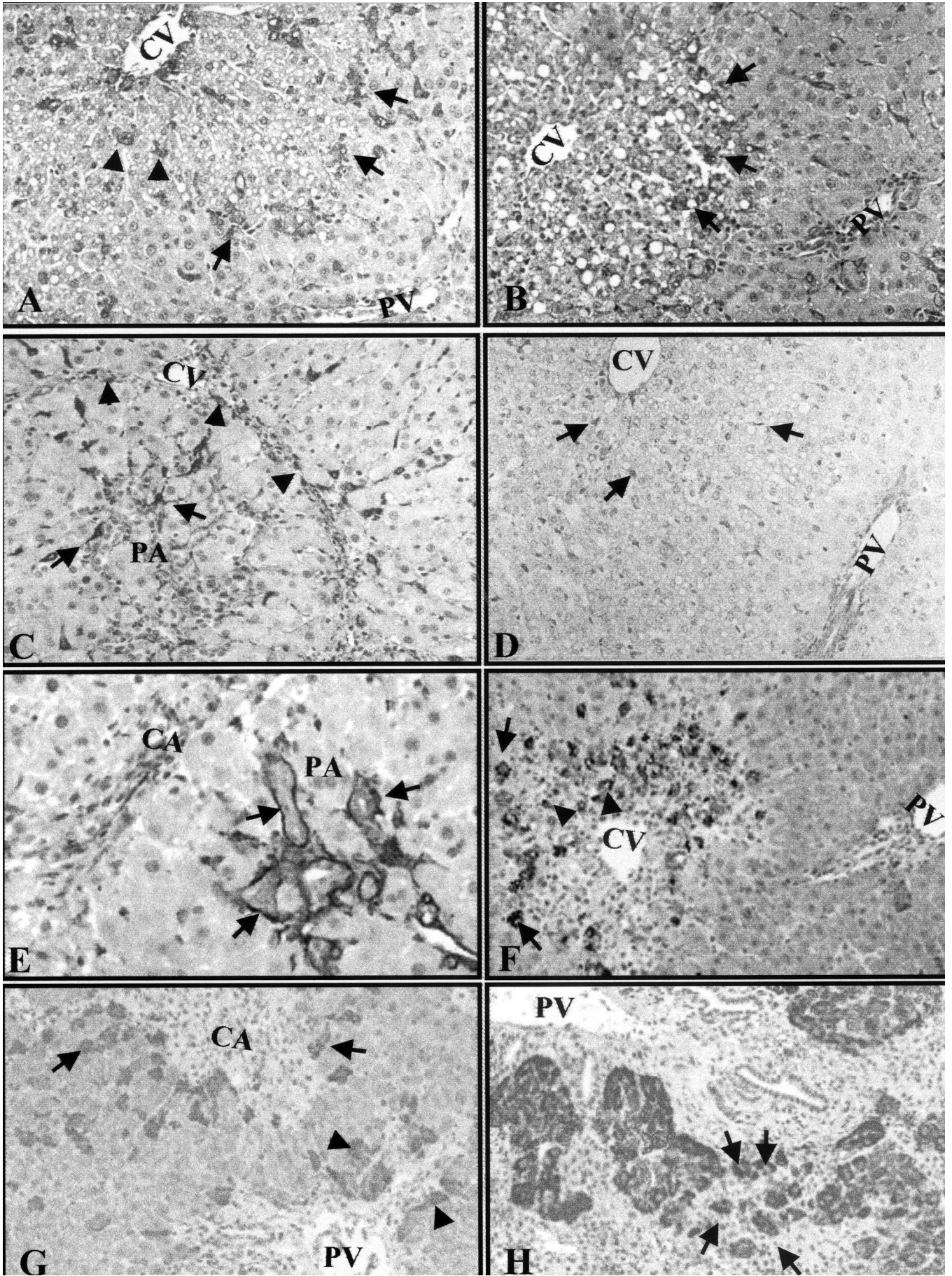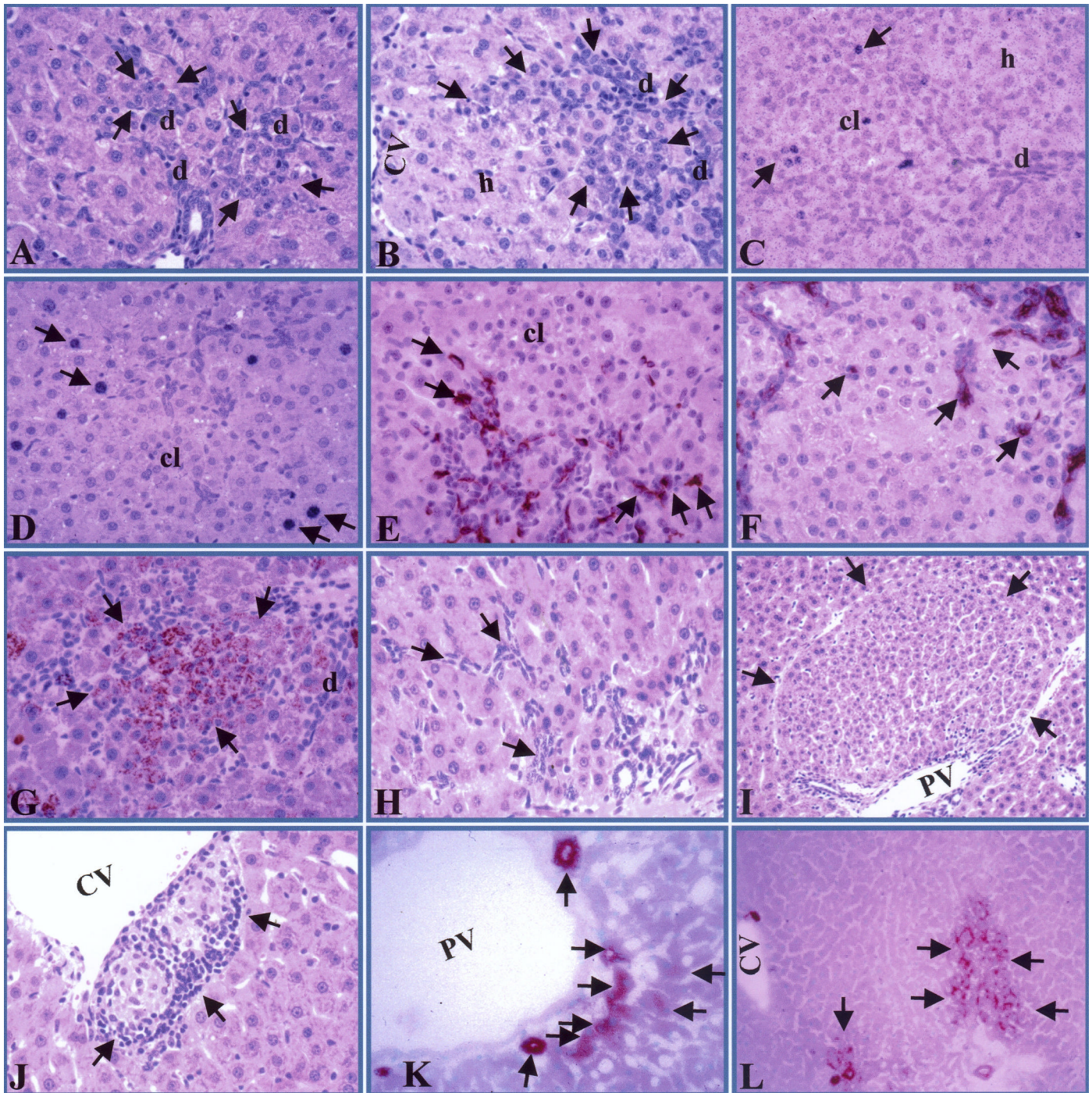
Fig. 5. Examples of small hepatocyte clusters and changes seen after day 7. **A.** Day 7, H & E. The arrows delineate two microscopic clusters of small hepatocytes located next to ductules (d). x 40. **B.** Day 8, H&E. The arrows delineate a larger cluster of small hepatocytes next to ducts (d). cv: central vein; h: hepatocyte. x 40. **C.** Day 8, autoradiograph. The arrows point to labeled small hepatocytes in a cluster (cl). d: ductules; h: hepatocytes. x 40. **D.** Day 21, autoradiograph. A cluster (cl) of small hepatocytes is surrounded by labeled hepatocytes. Labeled hepatocytes are seen from day 7 through day 28. x 40. **E.** Day 10, AFP. The arrows point to small hepatocytes containing AFP between AFP positive ductules and a cluster (cl) of small hepatocytes which do not contain AFP. x 40. **F.** Day 10, OV-6. he arrows pointing to the right mark individual cells (small hepatocytes or terminal duct cells?) positive for OV-6. The arrow pointing to the left marks an OV-6 negative hepatocyte next to and OV-6 positive terminal duct cell. x 40. **G.** Day 8, CPS-I. The arrows delineate a cluster of CPS-I positive small hepatocytes next to a ductule (d). x 40. **H.** Day 21, H&E. The arrows point to residual ducts. There are only a few remaining small hepatocytes at this time and clusters are not seen. In addition the ducts are now negative for AFP. x 40. **I.** 14 months, H&E. The arrows delineate a small nodule. These are seen from 2 to 14 months. x 20. **J.** 3 months. H&E. The arrows point to a microgranuloma next to the central vein (cv). A few small granuloma are seen from 2 months to 14 months. x 40. **K.** 3 months, GGT. The vertical arrow points to a GGT positive bile ducts. The horizontal arrows point to four hepatocytes in the limiting plate that are positive for GGT. x 40. **L.** 4 months, GGT. he vertical arrow points to positive bile ducts. The horizontal arrow delineate a GGT positive focus. A very few (one or two per liver sections) small GGT positive foci are seen from 3 to 14 months. x 20

periportal zone of hepatic lobule, in some sections to midzone, but few small hepatocytes remain (Fig. 5H). Both the intraportal ducts and the ductules which extend into the periportal zone are negative for AFP. Both the intraportal ducts and periportal ductules are GGT positive. At 3 months and 5 months, the ductules extend much less, only into immediately adjacent periportal zone, and small liver cells are difficult to find. At 14 months, there are a few foci of small eosinophilic cells, from 1 per 2 10x fields to 1 per 15 10x fields, some with a cribriform arrangement (Fig. 5I), but negative for OV-6, AFP and CPS-I. These foci contain from 100 to 1,000 cells on cross section. Rare microgranulomas are present in the central zone at all time points (Fig. 5J). Desmin is present around the intraportal ducts and in some stellate cells in the microgranulomas, but in contrast to the newly formed ductules, it is not present in the periportal ductules at these later times. After 2 months, both intraportal ducts and neoductules, as well as a few adjacent hepatocytes usually located at the limiting plate, are positive for GGT (Fig. 5K). Small foci of GGT positive cells are seen after 3 months (Fig. 5L).

Discussion

When hepatocyte proliferation is inhibited by AAF, centrolobular necrosis induced by CCl_4 stimulates reactive proliferation of bile ductules which expand and arborize across the hepatic lobule, in some instances reaching almost to the central vein by 7 days after induction of injury. In contrast, acute centrolobular injury induced by CCl_4 alone is repaired by proliferation of midzonal hepatocytes and migration of the expanding hepatocyte population into the necrotic tissue (Stowell and Lee, 1950; Abelev et al., 1979; Engelhardt et al., 1984; Tournier et al., 1988). When hepatocyte proliferation is inhibited, there is a prolonged process of proliferation of ducutlar cells into the hepatic lobule. The liver lobule structure is distorted by the expansion of ductules into the portal and midzones as the surviving hepatocytes, previously in the midzone, are "pushed" or "migrate" into the central necrotic zone. After the first 3 days, proliferation is predominantly in expanding ductules. When AAF treatment is discontinued on day 7, there appears to be rapid differentiation of cells at the end of the expanding ducts into clusters of small hepatocytes, as well as proliferation of surviving hepatocytes. Before day 7, few, if any, radiolabeld hepatocytes (S-phase cells) are seen, but from day 8 to 28, 4 to 10 labeled hepatocytes per 20x field are seen. This is consistent with the results of Ghoshal et al. (1983), who reported massive hepatocyte proliferation after termination of feeding AAF in a similar model, with disappearance of oval cells. However, our studies suggest that repair of the damaged central zone involves both hepatocyte proliferation and differentiation of ductular progenitor cells (oval cells) into liver cells. The differentiation of the ductule cells into liver cells is supported by the appearance of AFP in terminal duct cells and adjacent small hepatocytes, as well as the appearance of AFP in some larger hepatocytes near the proliferating ductules. In addition, the presence of clusters of CPS-I+ small hepatocytes (transitional hepatocytes?) (Lamers et al., 1984) next to the expanding proliferating ducts is consistent with terminal ductular cells or oval cells differentiating into hepatocytes.

These findings are consistent with other injury and carcinogenesis models which demonstrate the plasticity of small ductal and periductal cells in the liver (for review see Sell, 2001). Using the full Solt-Farber model, Novikoff et al. (1996) identified "blast" cells in the proliferating ductules which they concluded represented "stem" cells. Although there is some difference of opinion on whether the so-called "oval cells" all arise from ductal progenitor cells or also from a putative periductal liver stem cell (Evarts et al., 1987; Sell and Dunsford, 1989; Sell, 1990; Alterman, 1992; Thorgeirsson et al., 1993; Coleman et al., 1997; Alison et al., 1997a,b; Paku et al., 2001), there is general agreement that the oval cells induced by injury are able to differentiate into either biliary cells or hepatocytes, and in some cases, such as after furan injury, into gastrointestinal or pancreatic acinar cells (Elmore and Sirica, 1992; Sirica, 1996). In fact, two small microscopic areas of intestial metaplasia were seen on day 14 in the present experiment, but this was not a substantial feature. Thus, there seems little doubt that the liver contains progenitor cells located in the biliary system, either within or just outside intraportal ducts (Sell, 2001). The observation of loss of desmin around the intrahepatic ducts early in the proliferation process leaves open the possibility that duct cells may be able to migrate out of the ducts into the adjacent hepatic tissue. On the other hand, during the first two days after injury, small intraportal periductular cells also proliferate. These are similar to those described previously during hepatocarcinogenesis when hepatocyte proliferation is inhibited (Sell et al., 1981; Sell and Salman, 1984). The ability of agents which damage bile ducts, such as 4,4'-diaminodiphenylmethane (DDPM), to inhibit oval cell activation after CCl_4 induced necrosis in AAF treated rats, has been used as evidence that oval cell arise from bile ducts (Petersen et al., 1997). However, it is not known if DDPM treatment also affects periductular cells and DDPM, although a potent stimulator of biliary cell proliferation, does not induce classic oval cell proliferation (Sell, 1983). On the other hand, dexamethasone inhibits proliferation of hepatocytes and oval cells after AAF and partial hepatectomy, but not proliferation of bile duct cells (Nagy et al., 1998), suggesting that oval cells and hepatocytes may share growth regulatory mechanisms not found in bile duct cells.

The pattern of the restitutive response to hepatocyte loss varies markedly in different experimental models (Sell, 1998). After partial hepatectomy, the hepatocytes in the liver remnant proliferate to restore the liver mass,

and there is little or no evidence of involvement of a precursor or stem cell (Grisham, 1962; Bucher, 1963; Rabes et al., 1976). After centrolobular injury induced by CCl_4 (Stoval and Lee, 1950; Abelev et al., 1979; Engelhardt et al., 1984; Tournier et al., 1988) or galactosamine (Tournier et al., 1988; Lemire et al., 1991; Dabeva and Shafritz, 1993), the central necrotic zone is essentially restored by proliferation and migration of adjacent hepatocytes into the necrotic zone. There is marked proliferation of hepatocytes, but also a small component of proliferation of intraportal oval cells (stem cells?). Perhaps one of the most striking contrasts is between repair of periportal necrosis induced by allyl alcohol (AA) and the periportal proliferation seen in the present model (AAF/CCl_4). AA induced periportal necrosis is rapidly (within 5 to 7 days) restored by proliferation of small intraportal cells which expand in number and migrate across the necrotic zone (Yavorkovsky et al., 1995; Sell, 1997). During this process the putative progeny of the small periductular oval cells acquire markers and ultrastructural appearance of developing hepatocytes. There is very little ductal proliferation and this is limited to the intraportal zone. In contrast, in the present model there is clearly predominant ductal cell proliferation with expansion and arborization of ducts across the periportal zone. There is also, however, evidence of differentiation of oval cells into hepatocytes at the margins of the terminal ducts and hepatic cells. Thus, inhibition of hepatocyte proliferation by AAF results in prominent ductal proliferation in the CCl_4 injury model. In contrast, Petersen et al. (1998) describe more prominent ductal proliferation after AA injury than after CCl_4 injury, when hepatocyte proliferation is inhibited by AAF. It is possible that AAF may also inhibit hepatocyte differentiation or proliferation of hepatocyte lineage precursor cells after AA injury, resulting in enhanced and continued proliferation of ductular cells. It is not clear why Petersen et al. (1998) obtain less ductal response after CCl_4, as ductal proliferation is striking and predominant in the present study. The many different models of experimental liver injury are matched by different patterns of proliferation in human atypical ductular reactions (Sell, 1983).

The present study clearly identifies bile ductular cells as liver progenitor cells. However, the presence of a periductular cell with stem cell properties implies a possible different origin. Recent studies demonstrate that cells from the bone marrow (Petersen et al., 1999; Theise et al., 2000a), most likely primitive stem cells (Lagasse et al., 2000), may give rise to liver cells after transplantation in experimental models. In human female recipients of male bone marrow, 4 to 40% of hepatocytes and cholangioles contain the Y chromosome (Theise et al., 2000b); lower percentages (0.5 to 2%) are reported in another study (Alison et al., 2000). If bone marrow derived stem cells enter the liver and contribute to hepatocyte renewal, they would enter through the portal vasculature and locate next to the ducts in the portal

triad. Thus, it appears that the periductular non-descript cell which proliferates in response to periportal AA-induced injury and following exposure to carcinogens in a choline deficient diet, is a likely candidate for a bone marrow derived liver stem cell. If true, then these cells would represent a different level of renewing cells in the liver; the periductular cells being primitive stem cells and the ductular cells more restricted progenitor cells (Van der Kooy and Weiss, 2000; Sell, 2001). It is possible that stem cell in the bone marrow may localize to any organ under conditions of stress and contribute to reconstitution of loss of tissue cells (Van der Kooy, 2000). It is also possible that putative cells in one organ may relocate to another organ. Could liver stem cells recirculate to pancreas or to bone marrow or to other tissues? This question remains unanswered.

The interplay of different "littoral" cell types in liver restitution and oval cell proliferation is receiving increasing attention (Alison et al., 1996; Grisham and Thorgeirsson, 1997; Sell and Ilic, 1997). In the present model, the central necrotic zone appears to be cleared mainly through the presence of ED1 positive macrophages. ED2 positive Kupffer cells and desmin positive stellate cells migrate along with hepatocytes into the necrotic zone, most likely contributing to the clearing process, as well as providing extracellular matrix for the reconstruction of hepatic cords. Kupffer cells and macrophages are mainly phagocytic cells, but also synthesize and secrete a number of cytokines, including TNF- , IL-1 and IL-6 (Decker, 1990; McKuskey, 1993; Fausto, 1995; Gressner, 1998). Each of these is a powerful activator of acute phase protein synthesis and in this way may function to limit tissue damage. TNF- also enhances phagocytosis and lipogenesis and may be responsible for lipid accumulation seen in surviving hepatocytes in the necrotic zone. IL-1 also suppresses the function of the cytochrome P450 system, but, in addition, activates lymphocyte proliferation and hematopoiesis. IL-6 may stimulate fibroblast proliferation and contribute to scarring. Thus, Kupffer cells appear to be involved in the repair process mainly through controlling the extent of injury and preparing the tissue for regrowth of liver lineage cells, but it is unlikely that Kupffer cell or macrophage cytokines affect oval cells as oval cells do not have receptors for TNF- , IL-1 or IL-6 (Alison, 1996). Little, if any, fibrogenesis is seen in this process, suggesting that stellate cells are not activated to develop into myofibroblasts (Gressner, 1998).

Stellate (Ito) cells appear to play a prominant role in oval cell proliferation, migration, differentiation and ductal organization. Stellate cell transformation into myofibroblasts is mediated by cytokines released from inflammatory cells, primarily TGF- , which is produced by activated Kupffer cells and macrophages. However, at least during the time period studied, this effect is not seen, either because the appropriate fibrogenic factors are not produced or there is insufficient time for "activation" of stellate cells to myofibroblasts. However,

the close association of stellate cells and oval cells during oval cell growth and duct formation has suggested to Alison et al. (1996) that stellate cells are primarily involved in formation of ductules, as they surround reactive ductules in both human lesions and ductular reactions in animals (Martinez-Hernandez and Amenta, 1995). In addition, stellate cells likely provide growth factors for oval cells (Alison et al., 1996), as well as stimulate production of extracellular matrix (laminin and desmin) for reestablishing sinusoidal networks and factors for hepatocyte differentiation (Alison et al., 1996; Nagy et al., 1996). In the present studies, after days 2 and 3 the arborizing ducts become increasingly surrounded by a layer of desmin and laminin. These are also most likely produced by the adjacent stellate cells. However, expanding ductal cells after day 3 also appear to become increasingly positive for laminin, but not for desmin. The production of laminin is consistent with the concept that liver precursor cells may express products of less mature liver cells. Neonatal hepatocytes cultured in vitro in the presence of epidermal growth factor acquire a mesenchymal phenotype, including the production of vimentin (Pagan et al., 1997). This raises the possibility that the proliferating ductular cells may be able to synthesize some of their own ECM components. As described above, stellate cells also appear, along with Kupffer cells, to contribute extracellular matrix of the reforming hepatic cords in the necrotic central zone. After day 2, desmin positive cells are increasingly prominent in the necrotic zone, where they also appear to be contributing to the scaffold for the ingrowing hepatocytes, but then decrease as this zone is repaired.

References

Abelev G.I., Engelhardt N.V. and Elgort D.A. (1979). Immunochemical and immunohistochemical micromethods in the study of tumor-associated embryonic antigens (alpha-fetoprotein). Methods Cancer Res. 18, 1-37.

Alison M.R. (1986). Regulation of hepatic growth. Physiol. Rev. 66, 499-541.

Alison M.R., Golding M.N.C. and Sarraf C.E. (1996). Pluripotential liver stem cells: facultative stem cells located in the biliary tree. Cell Prolif. 29, 373-402.

Alison M., Golding M., Lalani E-N., Nagy P., Thorgeirsson S.S. and Sarraf C. (1997a). Wholesale hepatocytic differentiation in the rat liver from ductular oval cells, the progeny of biliary stem cells. J. Hepatol. 26, 343-352.

Alison M.R., Golding M. and Sarraf C.E. (1997b). Liver stem cells: when the going gets tough they get going. Int. J. Exp. Pathol. 78, 365-381.

Alison M.R., Poulsom R., Jeffery R., Dhillon A.P., Quaglia A., Jacob J., Novelli M., Prentice G., Williamson J. and Wright N.A. (2000). Hepatocytes from non-hepatic stem cells. Nature 406, 257.

Aterman K. (1992). The stem cells of the liver - selective review. J. Cancer Res. Clin. Oncol. 118, 87-115.

Armbrust T. and Ramadori G. (1996). Functional characterization of two different Kupffer cell populations of normal rat liver. J. Hepatol. 25, 518-528.

Ballardini G., Groff P., Giorgi L.B.D., Schuppan D. and Bianchi F.B. (1994). Ito cell heterogeneity: desmin-negative Ito cells in normal rat liver. Hepatology 19, 440-446.

Beck K., Hunter I. and Engel J. (1990). Structure and function of laminin: anatomy of a multidomain glycoprotein. FASEB J. 4, 148-160.

Bisgaard H.C., Nagy P., Ton P.T., Hu Z. and Thorgeisson S.S. (1994). Modulation of keratin 14 and -fetoprotein expression during hepatic oval cell proliferation and liver regeneration. J. Cell. Physiol. 159, 475-484.

Bisgaard H.C., Parmelee D.C., Dunsford H.A., Sechi S. and Thorgeisson S.S. (1993). Keratin 14 protein in cultured nonparenchymal rat hepatic epithelial cells: characterization of keratin 14 and keratin 19 as antigens for the commonly used mouse monoclonal antibody OV-6. Mol. Carcinogen. 7, 60-66.

Bisgaard H.C. and Thorgeisson S.S. (1991). Evidence for a common cell of origin for primitive epithelial cells isolated from rat liver and pancreas. J. Cell. Physiol. 147, 333-343.

Bucher N.L.R. (1963). Regeneration of mammalian liver. Int. Rev. Cytol. 15, 245-300.

Bucher N.L.R. and Malt R.A. (1971). Regeneration of the Liver and Kidney. Little, Brown and Co. Boston.

Coleman W.B., McCullough K.D., Esch G.L., Faris R.A., Hixson D.C., Smith G.J. and Grisham J.W. (1997). Evaluation of the differentiation potential of WB-F344 rat liver epithelial stem-like cells in vivo. Am. J. Pathol. 151, 353-359.

Crosby H.A., Hebscher S., Fabris L., Joplin R., Sell S., Kelly D. and Strain A.J. (1998). Immunolocalization of putative human liver progenitor cells in livers from patients with end-stage primary biliary cirrhosis and sclerosing cholangitis using the monoclonal antibody OV-6. Am. J. Pathol. 152, 771-779.

Dabeva M.D. and Shafritz D.A. (1993). Activation, proliferation and differentiation of progenitor cells into hepatocytes in the D-galactosamine model of liver regeneration. Am. J. Pathol. 143, 1606-1620.

Decker K. (1990). Biologically active products of stimulated liver macrophages (Kupffer cells). Eur. J. Biochem. 192, 245-261.

Dijkstra C.D., Dopp E.A., Jolong P. and Kraal G. (1985). The heterogeneity of mononuclear phagocytes in lymphoid organs: distinct macrophage subpopulations in the rat recognized by monoclonal antibodies ED1, ED2 and ED3. Immunology 54, 589-599.

Dunsford H.A., Karnasuta C., Hunt J.M. and Sell S. (1989). Monoclonal antibodies identify different lineages of chemically induced hepatocellular carcinoma in rats. Cancer Res. 49, 4894-4900.

Dunsford H.A. and Sell S. (1989). Production of monoclonal antibodies to preneoplastic liver cell populations induced by chemical carcinogens in rats to transplantable Morris hepatomas. Cancer Res. 49, 4887-4893.

Elmore L.W. and Sirica A.E. (1992). Sequential appearance of intestinal mucosal cell types in the right and caudate liver lobes of furan-treated rats. Hepatology 16, 1220-1226

Engel J. (1991). Laminin and other strange proteins. Biochemistry 31, 10643-10651.

Engelhardt N.V., Baranov V.N., Zareva M.N. and Goussov A.I. (1984). Ultrastructural localization of -fetoprotein (AFP) in regenerating

mouse liver poisoned with CCl$_4$: reexpression of AFP in differentiated hepatocytes. Histochemistry 80, 401-407.

Evarts R.P., Nagy P., Marsden E. and Thorgeirsson S.S. (1987). A precursor-product relationship exists between oval cells and hepatocytes in rat liver. Carcinogenesis 8, 1737-1740.

Fausto N., Laird A.D. and Webger E.M. (1995). Role of growth factors and cytokines in hepatic regeneration. FASEB J. 9, 1527-1536.

Geerts A., Bleser P.D., Hautekeete M.L., Niki T. and Wisse E. (1994). Fat-storing (Ito) cell biology. In: The Liver: Biology and pathology. Arias I.M., Boyer J.L., Fausto N., Jakoby W.B., Schachter D.A. and Shafritz D.A. (eds). Raven Press. New York. pp 819-838.

Germain L., Blouin M.J. and Marceau N. (1988). Biliary epithelial and hepatocytic cell lineage relationships in embryonic rat liver as determined by the differential expression of cytokeratins, -fetal protein, albumin and cell surface-exposed components. Cancer Res. 48, 4909-4918.

Ghoshal A.K., Mullen B., Medline A. and Farber E. (1983). Sequential analysis of hepatic carcinogenesis. Regeneration of liver after carbon tetrachloride-induced liver necrosis when hepatocyte proliferation is inhibited by 2-acetylaminofluorene. Lab. Invest. 48, 224-230.

Gijssel H.E.V., Ohlson L.C.E., Torndal U-B., Mulder G.J., Eriksson L.C., Porsch-Hallstrom I. and Meerman J.H.N. (2000). Loss of nuclear p53 protein in preneoplastic rat hepatocytes is accompanied by mdm-2 and bcl-2 overexpression and by defective response to DNA damage in vivo. Hepatology 32, 701-710.

Gressner A.M. (1998). The cell biology of liver fibrogenesis - an imbalance of proliferation, growth arrest and apotosis of myofibroblasts. Cell Tissue Res. 292, 447-452.

Grisham J.W. (1962). A morphologic study of deoxyribonucleic acid synthesis and cell proliferation in regenerating rat liver. Autoradiography with thymidine-H^3. Cancer Res. 22, 842-849.

Grisham J.R. and Thorgeirsson S.S (1997). Liver Stem cells. In: Stem cells. Potten C.S. (ed). Academic Press. New York. pp 233-282.

Koch K.S. and Leffert H.L. (1994). Hepatic regeneration and gene expression: a tribute to Hidematsu Hirai. J. Tumor Marker Oncol. 9, 35-56.

Lagasse E., Connors H., Al-Dhalimy M., Reitsma M., Dohse M., Osborne L., Wang X., Finegold M., Weissman I.L. and Grompe M. (2000). Purified hematopoietic stem cells can differentiatie into hepatocytes in vivo. Nature Med. 6, 1229-1234.

Lamers W.H., Zonneveld D. and Charles R. (1984). Inducibility of carbamoylphosphate synthetase (ammonia) in cultures of embryonic hepatocytes: ontogenesis of the responsiveness to hormones. Dev. Biol. 105, 500-508.

Lemire J.M., Shiojiri N. and Fausto N. (1991). Oval cell proliferation and the origin of small hepatocytes in liver injury induced by D-galactosamine. Am. J. Pathol. 139, 535-552.

Lindeman B., Skarpen E., Oksvold M.P. and Huitfeldt H.S. (2000). The carcinogen 2-acetylaminofluorene inhibits activation and nuclear accumulation of cyclin-dependent kinase 2 in growth-induced rat liver. Mol. Carcinogen. 27, 190-199.

Lindeman B., Skarpen E., Thorensen G.H., Christoffersen T., Wierod L., Madshus I.H. and Huitfeld H.S. (1999). Alteration of G1 cell-cycle protein expression and induction of P53 but not p21/waf1 by the DNA-modifying carcinogen 2-acetylaminofluorene in growth-stimulated hepatocytes in vitro. Mol. Carcinog. 24, 36-46.

Lombardi B. (1982). On the nature, properties and significance of oval cells. Recent Trends Chem. Carcinog. 1, 37-56.

Marceau N. (1990). Cell lineages and differentiation programs in epidermal, urothelial and hepatic tissues and their neoplasms. Lab. Invest. 63, 4-20.

Marceau N. (1994). Epithelial cell lineages in developing, restoring and transforming liver: evidence for the existence of a differentiation window. Gut 35, 294-296.

Marceau N., Blouin M.J., Noel M. and Torok N. (1992). The role of bipotential progenitor cells in liver ontogenesis and neoplasia. In: The role of cell types in hepatocarconogenesis. Sirica A.E. (ed). CRC Press. Boca Raton. pp 121-150.

Martinez-Hernandez A. and Amenta P. (1995). The extracellular matrix in hepatic regeneration. FASEB J. 9, 1401-1406.

McKuskey R.S. (1993). Endothelial cells and Kupffer cells. In: Molecular and cell biology of the liver. LeBouton A.V. (ed). CRC Press. Boca Raton. pp 407-427.

Nagy P., Bisgaard H.C., Santoni-Rugiu E. and Thorgeirsson S.S. (1996). In vivo infusion of growth factors enhances the mitogenic response of rat ductal (oval) cells after administration of 2-acetylaminofluorene. Hepatology 23, 71-79.

Nagy P., Kiss A., Schnur J. and Thorgeirsson S.S. (1998). Dexamethasone inhibits the proliferation of hepatocytes and oval cells but not bile duct cells in rat liver. Hepatology 28, 423-429.

Nostrant T.T., Miller D.L., Appelman H.D. and Cumucio J.J. (1978). Acinar distribution of liver cell regeneration after selective zonal injury in the rat. Gastroenterology 75, 181-186.

Novikoff P.M., Yam A. and Oikawa I. (1996). Blast-like compartment in carcinogen-induced proliferating bile ductules. Am. J. Pathol. 148, 1473-1492.

Ohlson L.C.E., Koroxenidou L. and Hallstrom I.P. (1998). Inhibition of in vivo rat liver regereration by 2-acetylamionfluorene affects the regulation of cell cycle-related proteins. Hepatology 27, 691-696.

Pagan R., Martin I., Llobera M. and Vilareo S. (1997). Epithelial-mesenchymal transition of cultured rat neonatal hepatocytes is differentailly regulated in response to epidermal growth factor and dimethyl sulfoxide. Hepatology 25, 598-606.

Paku S., Schnur J., Nagy P. and Thorgeirsson S.S. (2001). Origin and structural evolution of the early proliferatin oval cells in rat liver. Am. J. Pathol. 158, 1313-1323.

Paulsson M. (1992). Basement membrane proteins: structure, assembly, and cellular interactions. Crit. Rev. Biochem. Mol. Biol. 27, 93-127.

Petersen B.E., Zajac V.F. and Michalopoulos G.K. (1997). Bile ductular damage induced by methylene dianiline inhibits oval cell activation. Am. J. Pathol. 151, 905-909.

Petersen B.E., Zajac V.F. and Michalopoulos G.K. (1998). Hepatic oval cell activation in response to injury following chemically induced periportal or pericentral damage in rats. Hepatology 27, 1030-1038.

Petersen B.E., Bowen, W.C,. Patrene K.D., Mars W.M., Sullivan A.K., Murase N., Boggs S.S. and Greenberger J.S. (1999). Bone marrow as a potential source of hepatic oval cells. Science 14, 1168-1170.

Piazza J.G. (1917). Zur Kenntnis der Wirkung von Allylverbindungen. Z. Exp. Pathol. Ther. 17, 318-342.

Rabes H.M., Wirsching R., Tuczek H.V. and Lseler G. (1976). Analysis of cell cycle compartments of hepatocytes after partial hepatectomy. Cell Tissue Kinet. 9, 517-532.

Rojkind M. and Greenwel P. (1994). The extracellular matrix of the liver. In: The Liver: Biology and pathology. Arias I.M., Boyer J.L., Fausto N., Jakoby W.B., Schachter D.A. and Shafritz D.A. (eds). Raven Press. New York. pp 843-868.

Rutenberg A.M., Kim H., Fischbein J.W., Hanker J.S., Wasserkrug H.L. and Seligman A.M. (1969). Histochemical and ultrastructural demonstration of -glutamyl transpeptidase activity. J. Histochem. Cytochem. 17, 517-526.

Sala-Trepat J.M., Dever J., Sargent T.D., Thomas K., Sell S. and Bonner J. (1979). Changes in expression of albumin and alphafetoprotein genes during rat liver development and neoplasia. Biochemistry 18, 695-699.

Sell S. (1973). Radioimmunoassay of -fetoprotein. Cancer Res. 33, 1010-1015.

Sell S. (1978). Distribution of alphafetoprotein and albumin containing cells in the livers of Fischer rats fed four cycles of N-2-fluorenylacetamide. Cancer Res. 75, 181-186.

Sell S. (1983). A comparison of oval cells induced in rat liver by feeding N-2-fluorenylacetamide in a choline-devoid diet and bile duct cells induced by feeding 4,4'-diaminodiphenylmethane. Cancer Res. 43, 1761-1767.

Sell S. (1990). Is there a liver stem cell? Cancer Res. 50, 3811-3815.

Sell S. (1994). Liver stem cells. Modern Pathol. 7, 105-112.

Sell S. (1997). Electron microscopic identification of putative liver stem cells and intermediate hepatocytes following periportal necrosis iduced in rats by allyl alcohol. Stem Cells 15, 378-385.

Sell S. (1998). Comparison of liver progenitor cells in human atypical ductular reactions with those seen in experimental models of liver injury. Hepatology 27, 317-331.

Sell S. (2001). Heterogeneity and plasticity of hepatocyte lineage cells and the origin of hepatocellular carcinoma. Hepatology 33, 738-750.

Sell S. and Dunsford H. (1989). Evidence for the stem cell origin of hepatocellular carcinoma and cholangiocarcinoma. Am. J. Pathol. 134, 1347-1362.

Sell S. and Ilic Z. (1997). Liver stem cells. R.G. Landes Company and Chapman & Hall. Austin, TX and New York.

Sell S. and Leffert H.L. (1982). An evaluation of the cellular lineages in the pathogenesis of experimental hepatocellular carcinoma. Hepatology 2, 77-86.

Sell S. and Ruoslahti E. (1982). Expression of fibronectin and laminin in the rat liver after partial hepatectomy, during carcinogenesis and in transplantable hepatocellular carcinomas. J. Natl. Cancer Inst. 69, 1105-1114.

Sell S. and Salman J. (1984). Light and electron microscopic autoradiographic analysis of proliferating cells during the early stages of chemical hepatocarcinogenesis induced by feeding N-2-fluorenylacetamide in a choline devoid diet. Am. J. Pathol. 114, 287-300.

Sell S., Becker F.F., Leffert H.L. and Watabe J. (1976). Expression of an oncodevelopmental gene product (alphafetoprotein) during fetal development and oncogenesis. Cancer Res. 36, 4239-4249.

Sell S., Osborn K. and Leffert H. (1981). Autoradiography of "oval cells" appearing rapidly in the livers of rats fed N-2-fluorenylacetamide in a choline devoid diet. Carcinogenesis 2, 7-14.

Sell S., Sala-Trepat J.M., Sargent T.D., Thomas K., Nahom J.L.,

Goodman T. and Bonner J. (1980). Molecular mechanisms of control of albumin and alphafetoprotein production: a system to study the early effects of chemical hepatocarcinogenesis. Cell Biol. Int. Rep. 4, 234-254.

Shinozuka H., Lombardi B., Sell S. and Iammarino R.M. (1978). Early histological and functional alterations of ethionine liver carcinogenesis in rats fed a choline-deficient diet. Cancer Res. 38, 1092-1098.

Shiojiri N., Lemire J.M. and Fausto N. (1991). Cell lineages and oval cell progenitors in rat liver development. Cancer Res. 51, 2611-2620.

Sirica A.E. (1996). Biliary proliferation and adaptation in furan-induced rat liver injury and carcinogenesis. Toxicol. Pathol. 24, 90-99.

Solt D.C., Medline A.C. and Farber E. (1977). Rapid emergence of carcinogen-induced initiated hyperplastic lesions in a new model for the sequential analysis of liver carcinogenesis. Am. J. Pathol. 88, 595-609.

Stowell R.E. and Lee C.S. (1950). Histochemical studies of mouse liver after single feeding of carbon tetrachloride. Arch. Pathol. 50, 519-537.

Theise N.D., Badve S., Saxena R., Henegariu O., Sell S., Crawford J.M. and Krause D.S. (2000a). Derivation of hepatocytes from bone marrow cells in mice after radiation-induced myeloablation. Hepatology 31, 235-240.

Theise N.D., Nimmakayalu M., Gardner R., Illei P.B., Morgan G., Teperman L., Henegariu O. and Krause D.S. (2000b). Liver from bone marrow in humans. Hepatology 32, 11-16.

Thorgeirsson S.S., Mitchell J.R., Sasame H.A. and Potter W.Z. (1976). Biochemical changes after hepatic injury by allyl alcohol and N-hydroxy-2-acetylaminofluorene. Chem-Biol. Interact. 15, 139-147.

Thorgeirsson S.S., Evarts R.P., Bisgaard H.C., Fujio K. and Hu Z. (1993). Hepatic stem cell compartment: activation and lineage commitment. Proc. Soc. Exp. Biol. Med. 204, 253-260.

Tournier I., Legres L., Schoevaert D., Feldman G. and Bernuau D. (1988). Cellular analysis of -fetoprotein gene activation during carbon tetrachloride and D-galactosamine induced acute liver injury in rats. Lab. Invest. 59, 657-665.

Trautwein C., Will M,. Kubicka S., Rakemann J., Flemming P. and Manns M.P. (1999). 2-acetylaminofluoerene blocks cell cycle progression after hepatectomy by p21 induction and lack of cyclin E expression. Oncogene 18, 6443-6453.

Van der Kooy D. and Weiss S. (2000). Why stem cells? Science 287, 1439-1441.

Wilson J.W. and Leduc E.H. (1958). Role of cholangioles in restoration of the liver of the mouse after dietary injury. J. Pathol. Bacteriol. 76, 441-449.

Yavorkovsky L., Lai E., Ilic Z. and Sell S. (1995). Participation of small intraportal "stem" cells in the restitutive response of the liver to periportal necrosis induced by allyl alcohol. Hepatology 21, 1702-1712.